

EARLY BLUE EXCESS FROM THE TYPE Ia SUPERNOVA 2017cbv AND IMPLICATIONS FOR ITS PROGENITOR

GRIFFIN HOSSEINZADEH^{1,2}, DAVID J. SAND^{3,4}, STEFANO VALENTI⁵, PETER BROWN⁶, D. ANDREW HOWELL^{1,2},
CURTIS MCCULLY^{1,2}, DANIEL KASEN^{7,8}, IAIR ARCAVI^{1,2,11}, K. AZALEE BOSTROEM⁵, LEONARDO TARTAGLIA^{3,4,5},
ERIC Y. HSIAO⁹, SCOTT DAVIS⁹, MELISSA SHAHBADEH⁹, AND MAXIMILIAN D. STRITZINGER¹⁰

¹Las Cumbres Observatory, 6740 Cortona Drive, Suite 102, Goleta, CA 93117-5575, USA; griffin@lco.global

²Department of Physics, University of California, Santa Barbara, CA 93106-9530, USA

³Department of Astronomy/Steward Observatory, 933 North Cherry Avenue, Rm. N204, Tucson, AZ 85721-0065, USA

⁴Department of Physics & Astronomy, Texas Tech University, Box 41051, Lubbock, TX 79109-1051, USA

⁵Department of Physics, University of California, 1 Shields Avenue, Davis, CA 95616-5270, USA

⁶Mitchell Institute for Fundamental Physics and Astronomy, Texas A&M University, College Station, TX 77843-4242, USA

⁷Nuclear Science Division, Lawrence Berkeley National Laboratory, Berkeley, CA 94720-8169, USA

⁸Departments of Physics and Astronomy, University of California, Berkeley, CA 94720-7300, USA

⁹Department of Physics, Florida State University, 77 Chieftain Way, Tallahassee, FL 32306-4350, USA

¹⁰Department of Physics and Astronomy, Aarhus University, Ny Munkegade 120, DK-8000 Aarhus C, Denmark

(Received 2017 June 27; Revised 2017 July 31; Accepted 2017 August 2; Published 2017 August 14)

ABSTRACT

We present very early, high-cadence photometric observations of the nearby Type Ia SN 2017cbv. The light curve is unique in that it has a blue bump during the first five days of observations in the U , B , and g bands, which is clearly resolved given our photometric cadence of 5.7 hr during that time span. We model the light curve as the combination of early shocking of the supernova ejecta against a nondegenerate companion star plus a standard SN Ia component. Our best-fit model suggests the presence of a subgiant star $56 R_{\odot}$ from the exploding white dwarf, although this number is highly model-dependent. While this model matches the optical light curve well, it overpredicts the observed flux in the ultraviolet bands. This may indicate that the shock is not a blackbody, perhaps because of line blanketing in the UV. Alternatively, it could point to another physical explanation for the optical blue bump, such as interaction with circumstellar material or an unusual nickel distribution. Early optical spectra of SN 2017cbv show strong carbon (C II $\lambda 6580$) absorption up through day -13 with respect to maximum light, suggesting that the progenitor system contains a significant amount of unburned material. These early results on SN 2017cbv illustrate the power of early discovery and intense follow-up of nearby supernovae to resolve standing questions about the progenitor systems and explosion mechanisms of SNe Ia.

Keywords: supernovae: general — supernovae: individual (SN 2017cbv)

1. INTRODUCTION

Type Ia supernovae (SNe Ia) are the thermonuclear explosions of carbon–oxygen white dwarfs and are standardizable candles vital for cosmological distance measurements. Despite intense study, the progenitor scenarios and explosion mechanisms for these events are still not understood, and may have multiple pathways (see [Howell 2011](#); [Maoz et al. 2014](#), for reviews). The two main progenitor pictures are the single-degenerate (SD) scenario, where the white dwarf accretes material from a nondegenerate secondary star ([Whelan & Iben 1973](#)), and the double-degenerate scenario (DD), where two white dwarfs are present in the pre-supernova sys-

tem ([Iben & Tutukov 1984](#); [Webbink 1984](#)). However, the details of both scenarios are still under investigation (e.g., [Pakmor et al. 2012](#); [Kushnir et al. 2013](#); [Shen & Bildsten 2014](#); [Levanon & Soker 2017](#)).

The early light curves of SNe Ia are promising ways to constrain the progenitor systems and the physics of the explosion. For instance, the collision of the SN ejecta with a nondegenerate companion star may manifest as an early blue or ultraviolet (UV) bump in the light curve, depending on the viewing angle ([Kasen 2010](#)). Early temperature or luminosity measurements can directly constrain the radius of the progenitor ([Piro et al. 2010](#); [Rabinak et al. 2012](#)); observed limits have confirmed that the exploding star must be a white dwarf (e.g., [Nugent et al. 2011](#); [Bloom et al. 2012](#); [Zheng et al.](#)

¹¹ Einstein Fellow

2013). Recently, Piro & Morozova (2016) explored how early SN Ia light curve behavior depends on the amount and extent of circumstellar material (CSM) and the distribution of ^{56}Ni in the ejecta, which is expected to vary considerably with the location(s) of ignition in the progenitor. Finally, different explosion mechanisms may also produce distinct early light curves (Noebauer et al. 2017).

Very early SN Ia light curve observations are becoming more common, and recent studies have shown that they display a range of early behaviors (Hayden et al. 2010; Bianco et al. 2011; Ganeshalingam et al. 2011; Brown et al. 2012a; Zheng et al. 2013, 2014; Cao et al. 2015; Firth et al. 2015; Goobar et al. 2015; Im et al. 2015; Marion et al. 2016; Zheng et al. 2017; Shappee et al. 2016b). iPTF14atg (Cao et al. 2015) and SN 2012cg (Marion et al. 2016) both showed early, UV/blue excesses in their light curves. iPTF14atg was an SN 2002es-like event, which are subluminous, do not follow the Phillips (1993) relation, have low velocities, and show Ti II absorption (Ganeshalingam et al. 2012). Cao et al. (2016) found that the UV excess in iPTF14atg was consistent with the SN ejecta interacting with a companion star, although Kromer et al. (2016) find the SD scenario incompatible with the observed spectral evolution. In SN 2012cg, a normal SN Ia, the early blue bump was again interpreted as a signature of ejecta-companion interaction, consistent with a $6 M_{\odot}$ main-sequence companion $29 R_{\odot}$ from the white dwarf, using the Kasen (2010) formulation.¹² However, Shappee et al. (2016a) find that other probes of the progenitor system do not support the SD interpretation for SN 2012cg.

Here, we present the early light curve and spectra of SN 2017cbv, which show a clear blue excess during the first several days of observations. This excess may be a more subtle version of that seen in SN 2012cg and iPTF14atg, but seen more clearly here thanks to denser sampling.

2. OBSERVATIONS AND DATA REDUCTION

SN 2017cbv (a.k.a. DLT17u) was discovered on MJD 57822.14 (2017 March 10 UT) at a magnitude of $R \approx 16$ by the Distance Less Than 40 Mpc survey (DLT40; L. Tartaglia et al. 2017, in preparation), a one-day cadence SN search using a PROMPT 0.4 m telescope (Reichart et al. 2005), and was confirmed by a second DLT40 image during the same night (Valenti et al. 2017). Our last nondetection was on MJD 57791. The SN is located on the outskirts of the nearby spiral galaxy NGC 5643. Within hours of discovery (MJD

57822.7), the transient was classified as a very young SN Ia with the robotic FLOYDS spectrograph mounted on the Las Cumbres Observatory (LCO; Brown et al. 2013) 2 m telescope in Siding Spring, Australia (Hosseinzadeh et al. 2017).

UBVgri follow-up observations were obtained with Sinistro cameras on LCO’s network of 1 m telescopes. Using `lcogtsnpipe` (Valenti et al. 2016), a PyRAF-based photometric reduction pipeline, we measured aperture photometry of the SN. Because the SN is bright and far from its host galaxy, image subtraction and PSF fitting are not required. Local sequence stars were calibrated to the L101 standard field observed on the same night at the same observatory site using *UBV* Vega magnitudes from Stetson (2000) and *gri* AB magnitudes from the SDSS Collaboration (2016).

The *Swift* satellite began observing SN 2017cbv on MJD 57822.52. Ultra-Violet Optical Telescope (UVOT; Roming et al. 2005) photometry is given in the UVOT Vega photometry system using the pipeline for the *Swift* Optical Ultraviolet Supernova Archive (SOUSA; Brown et al. 2014) and the zeropoints of Breeveld et al. (2010). Smaller hardware windows were used in the optical near maximum brightness in order to reduce coincidence loss and measure brighter magnitudes without saturation (Poole et al. 2008; Brown et al. 2012b). A few *U*- and *B*-band observations on the rising branch were saturated and are excluded.

Finally, we obtained absolute magnitudes by applying the distance modulus, $\mu = 31.14 \pm 0.40$ mag (16.9 ± 3.1 Mpc), of Tully (1988) and the Milky Way extinction corrections, $E(B - V) = 0.15$ mag, of Schlafly & Finkbeiner (2011). We assume no additional host galaxy extinction, given the SN’s position in the outskirts of NGC 5643 and a lack of narrow Na I D absorption in high-resolution spectra (D.J. Sand et al. 2017, in preparation).

Our photometry is shown in Figure 1. By fitting quadratic polynomials to the observed light curve, one around peak and one around +15 days, we find that SN 2017cbv reached a peak magnitude of $B = 11.72$ mag ($M_B = -20.04$ mag) on MJD 57841.07, with $\Delta m_{15}(B) = 1.06$ mag. The decline rate of SN 2017cbv is near the average for normal SNe Ia (see, e.g., Figure 14 of Parrent et al. 2014). The peak absolute magnitude appears to be on the bright end of SNe Ia (Parrent et al. 2014), but this is uncertain due to the poorly constrained distance to NGC 5643. All figures use MJD 57821 as the nominal explosion date (see §4).

3. LIGHT CURVE MORPHOLOGY AND FITTING

The very early light curve of SN 2017cbv shows a prominent blue bump in the *U*, *B* and *g* bands during the first five days of observation, also visible in its

¹² Note that the models of Kasen (2010) directly constrain the binary separation, not the companion mass. Masses can be inferred by assuming the companion is in Roche lobe overflow and applying a mass-radius relationship.

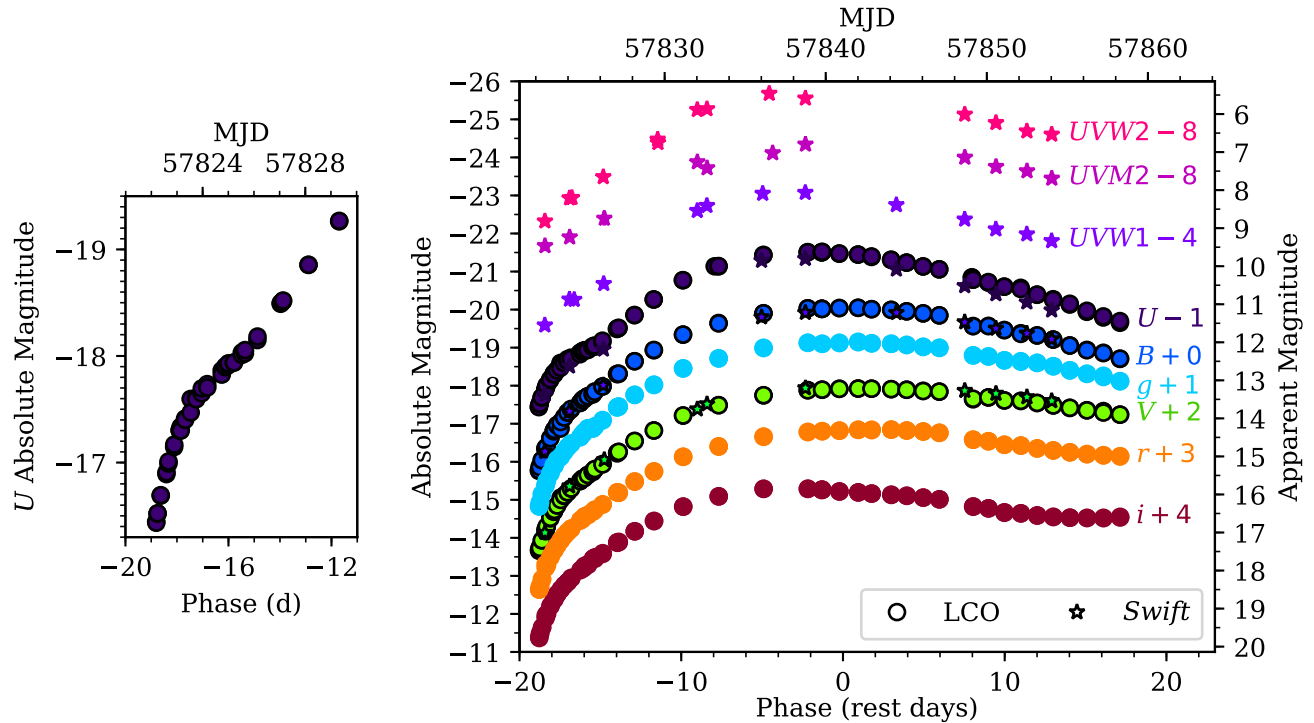


Figure 1. UV and optical photometry of SN 2017cbv, in absolute and extinction-corrected apparent magnitudes. The left panel shows a bump in the early U -band light curve. (The data for this figure are available.)

$U - B$ and $B - V$ colors (Figure 2). This indicates a high-temperature component of the early light curve in addition to the normal SN Ia behavior.

There are several possibilities for the origin of the early light curve bump (see §5 for a discussion), but here we fit the analytic models of Kasen (2010) for a nondegenerate binary companion shocking the SN ejecta, as might be expected from the SD scenario. While in reality such a collision would be highly asymmetric, we use Kasen’s analytic expressions for the luminosity within an optimal viewing angle. By further assuming that the shock consists of a spherical blackbody, Kasen arrives at the following equations for the photospheric radius and effective temperature¹³:

$$R_{\text{phot}} = (2700 R_{\odot}) x^{1/9} \kappa^{1/9} t^{7/9} \quad (1)$$

$$T_{\text{eff}} = (25,000 \text{ K}) a^{1/4} x^{1/144} \kappa^{-35/144} t^{-37/72} \quad (2)$$

where a is the binary separation in units of 10^{11} m ($144 R_{\odot}$), κ is the opacity in units of the electron scattering opacity (we fix $\kappa = 1$ in our fits), and t is the time since explosion in days. In addition, we define

$$x \equiv \frac{M}{M_{\text{Ch}}} \left(\frac{v}{10,000 \text{ km s}^{-1}} \right)^7, \quad (3)$$

where M is the ejected mass, $M_{\text{Ch}} = 1.4 M_{\odot}$ is the Chandrasekhar mass, and v is the transition velocity

between power laws in the density profile.

Our light curve model is the sum of the SiFTO template (Conley et al. 2008) to account for the normal SN Ia emission, and Kasen’s shock model to account for the blue excess. We scale each band of the SiFTO template independently. In the U , B , V , and g bands, we fix the scaling factor to match the observed peak. In the r and i bands, we leave the scaling factor as a free parameter in order to account for any contribution from the shock in those bands around peak (predicted for some combinations of parameters). We also allow the time of B -band maximum light and the stretch (Perlmutter et al. 1997) of the SiFTO template to vary.

In total, we have eight parameters:

1. The explosion time;
2. The binary separation, a ;
3. $x \propto Mv^7$ (Equation (3));
4. A factor on the r SiFTO template;
5. A factor on the i SiFTO template;
6. The time of peak;
7. The stretch; and
8. A factor on the shock component in U (see below).

We fit this combined model to our $UBVgri$ light curve from LCO using a Markov Chain Monte Carlo routine based on the `emcee` package (Foreman-Mackey et al. 2013). We cannot include the *Swift* data in the fit due to a lack of early UV SN Ia templates. In addition to the photometric uncertainty, we add a 2% systematic

¹³ Equation (2) corrects the exponent on κ in Kasen’s Equation (25).

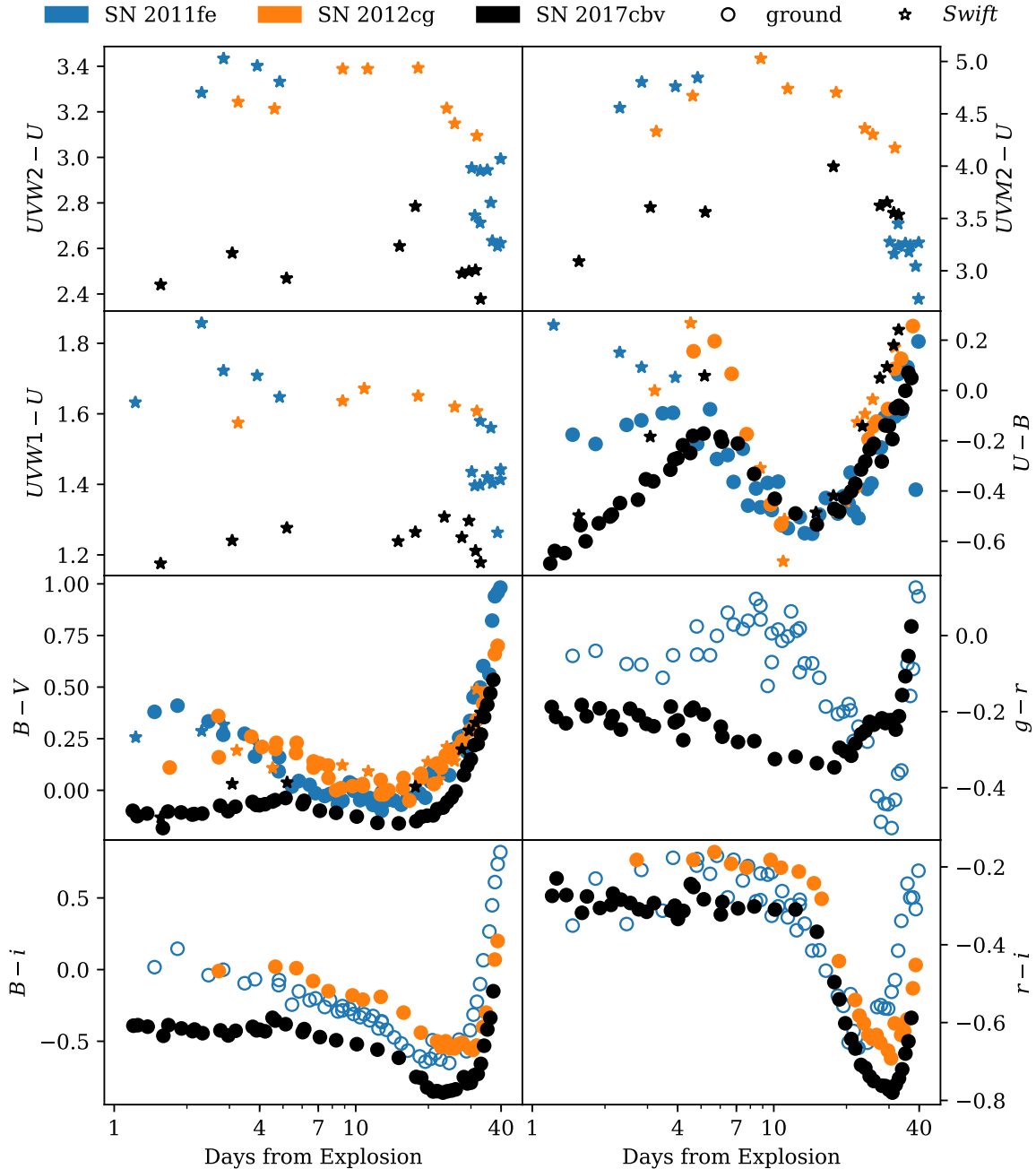


Figure 2. Milky Way extinction-corrected ultraviolet and optical colors of SN 2017cbv, compared to SN 2011fe (Zhang et al. 2016) and SN 2012cg (Marion et al. 2016). The colors of the subluminal SN Ia iPTF14atg are quite different than colors of the other events (Cao et al. 2015), so they are not shown. All *Swift* photometry is from SOUSA (Brown et al. 2014). Open circles indicate $V - R$, $B - I$, and $R - I$ colors that have been converted to $g - r$, $B - i$, and $r - i$, respectively, using the transformations of Jordi et al. (2006). Note the unusually blue $U - B$ and $B - V$ colors of SN 2017cbv during the bump (one to five days after explosion).

(0.02 mag) uncertainty in quadrature as an estimate for our calibration uncertainties. For each of our observations, we find the expected R_{phot} and T_{eff} at that time, calculate the corresponding average L_{ν} in each filter, and compare that to our measured L_{ν} .

One caveat to our approach is that the SiFTO template may not describe the early light curve behavior of normal SNe Ia correctly in all filters. Given the small number of events observed 10–20 days before peak, re-

liable templates do not exist at these phases. However, we are encouraged by the fact that our SiFTO-based results qualitatively agree with other template fitters that we experimented with—SALT2 (Guy et al. 2007), MLCS2k2 (Jha et al. 2007), and the observed light curve of SN 2011fe (Zhang et al. 2016)—even at these early times.

We find that the SiFTO+Kasen model provides an excellent fit to our ground-based data (reduced $\chi^2 = 8.6$

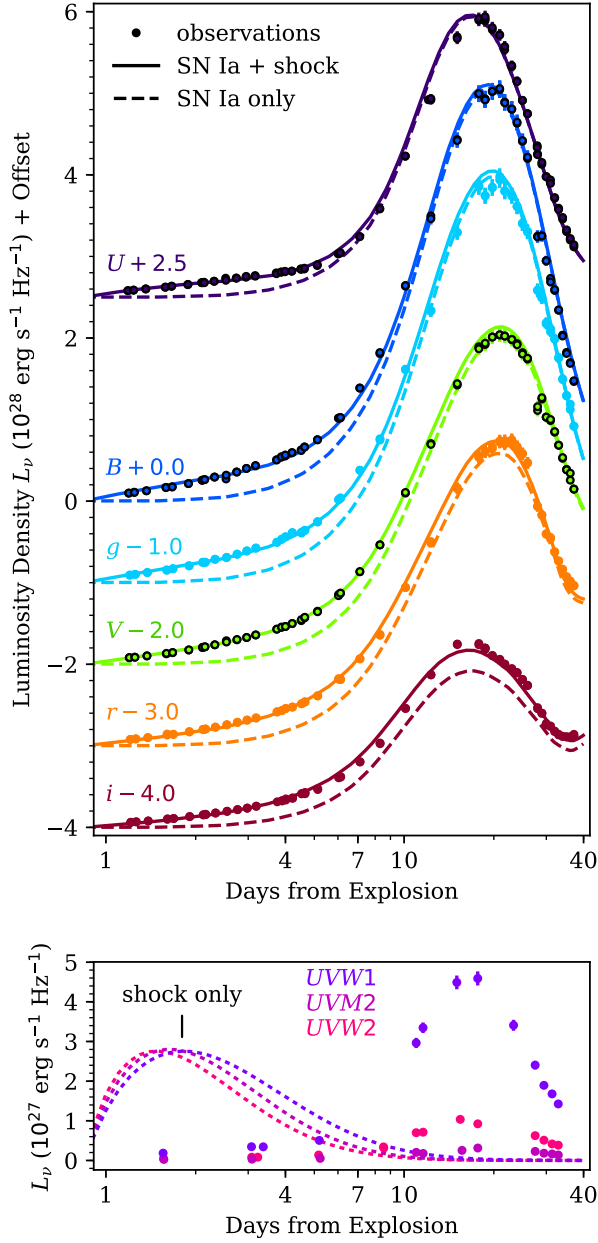


Figure 3. Best-fit model (solid lines), consisting of an SN Ia template (Conley et al. 2008) plus a companion shock component from Kasen (2010), to the ground-based light curve of SN 2017cbv. The dashed lines show the best-fit model with the companion shock subtracted. The model provides a good fit to the early light curve bump, but the shock model alone (dotted lines) overpredicts the early *UVW1* to *UVW2* luminosity.

after including our 2% calibration uncertainty), correctly predicting the blue bump at early times (Figure 3, top). Although at first glance our light curves do not look peculiar in the redder bands, emission from the shock model several weeks after explosion contributes to the observed luminosity around peak. Specifically, our best-fit model indicates that 5% and 15% of the *r*- and *i*-band peak luminosities, respectively, come from the shock component.

The best-fit binary separation is $56 R_{\odot}$, implying a stellar radius of $\sim 20 R_{\odot}$ (assuming Roche lobe overflow; Eggleton 1983). $56 R_{\odot}$ is among the largest binary separations for SD SN Ia progenitors from binary population synthesis calculations (Liu et al. 2015). However, this value is quite sensitive to the early color evolution of our SN Ia template. As these templates may not be valid 15–20 days before peak, this result should be treated with caution. Furthermore, our simplified spherical model ignores the degeneracy between binary separation (a) and viewing angle; a bright (large a) off-angle shock looks similar to a faint (small a) shock along the line of sight.

Given the strong dependence of x on the transition velocity ($\propto v^7$), which is not observable, we cannot robustly estimate the ejecta mass. However, taking our best-fit value of $x = 3.84 \pm 0.19$ and assuming a Chandrasekhar mass of ejecta, we find a reasonable transition velocity of $v \approx 12000 \text{ km s}^{-1}$ (subject to uncertainty in the distance modulus). The best-fit explosion time is MJD 57821.9, about 7 hr before discovery, and the best-fit time of *B*-band peak for the SiFTO component is MJD 57840.2. The best-fit stretch from the SiFTO template is 1.04.

Despite the success of the binary companion shock model in the optical, we required a scaling factor of 0.61 on the *U*-band shock component in order to fit the data. The *UVW1*, *UVM2* and *UVW2* emission are even further overpredicted by the shock model (Figure 3, bottom). We discuss the potential causes of this discrepancy in §5.

4. EARLY SPECTRA

We obtained several additional optical and near-infrared (NIR) spectra of SN 2017cbv with FLOYDS and the SpeX NIR spectrograph (Rayner et al. 2003) at the NASA Infrared Telescope Facility, a selection of which are presented in Figure 4. As the event is ongoing at the time of publication, the full data set and analysis will be presented elsewhere (D. J. Sand et al. 2017, in preparation). In summary, the spectrum of SN 2017cbv greatly resembles the spectrum of SN 2013dy (Zheng et al. 2013) during the two weeks before maximum light, with Si II and Ca II absorption features weaker than the prototypical Type Ia SN 2011fe but stronger than the somewhat overluminous SN 1999aa (Garavini et al. 2004). Despite the spectroscopic similarity to SN 2013dy, the light curve of SN 2017cbv declines slightly faster: $\Delta m_{15}(B) = 1.06 \text{ mag}$ for SN 2017cbv versus 0.92 mag for SN 2013dy (Pan et al. 2015).

We measure a Si II $\lambda 6355$ velocity of $22,800 \text{ km s}^{-1}$ in the initial spectrum of SN 2017cbv, 19 days before maximum light. The absorption feature just redward of Si II could either be a lower-velocity compo-

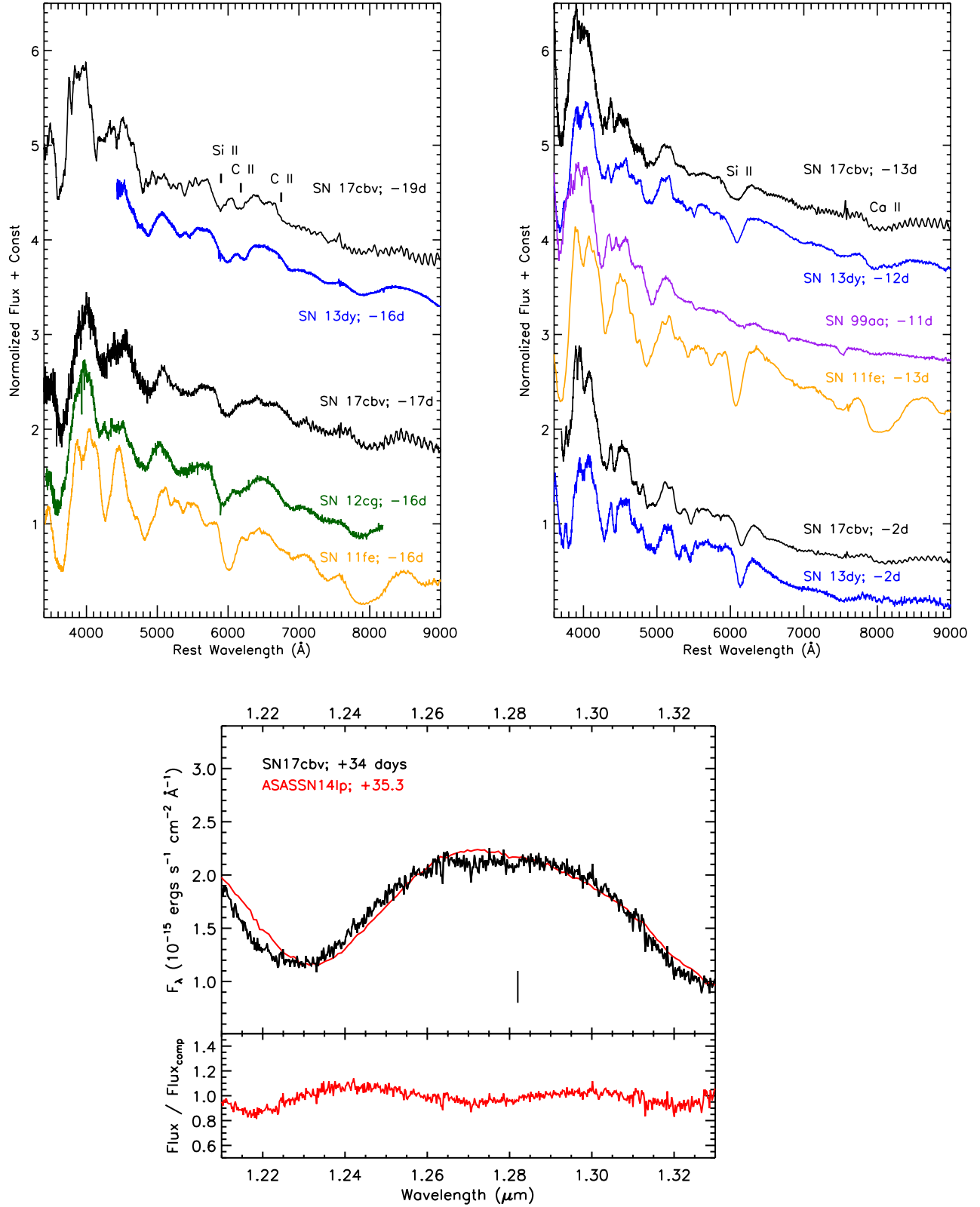


Figure 4. Top left: the smoothed -19 day spectrum of SN 2017cbv shows conspicuous carbon similar to SN 2013dy, which persists at least until day -17 . The -17 day spectrum is quite similar to the -16 day spectrum of SN 2012cg, which also showed an early blue bump in its light curve, but not the -16 day spectrum of SN 2011fe. Top right: spectra of SN 2017cbv at -13 and -2 days are very similar to SN 2013dy at similar epochs. Si II and Ca II are present and too strong to be SN 1999aa-like, but not as strong as in SN 2011fe. Bottom: NIR spectrum of SN 2017cbv in the region of Pa β (marked by the vertical line) compared to a spectrum of ASASSN-14lp. The bottom panel shows the ratio of the two spectra, yielding no evidence of narrow hydrogen emission from interaction with a companion star.

ment (9400 km s⁻¹) of the same line or C II λ 6580 at 19,800 km s⁻¹. We prefer the latter interpretation, as (1) it correctly predicts the tentative position of C II λ 7234 in the same spectrum and (2) 9400 km s⁻¹ would be uniquely low among very early SN Ia spectra (Silverman et al. 2012). The detection of unburned carbon can directly discriminate between the proposed SN Ia explosion mechanisms but is rarely seen in optical spectra even at these early times (Parrent et al. 2011; Silverman & Filippenko 2012), except for in super-Chandrasekhar SNe Ia (Howell et al. 2006). In SN 2017cbv, this feature disappears by day -13, reinforcing the need for early spectroscopy to fully account for unburned carbon.

The Si II absorption feature at -13 days clearly shows signs of two velocity components at 16,500 and 10,500 km s⁻¹. It is likely that the earlier spectra of SN 2017cbv are dominated by the high-velocity component of Si II, but we cannot fully trace the transition to low-velocity Si II due to our lack of FLOYDS spectra between -13 and -2 days. We note that -13 days was also the approximate epoch at which SN 2012fr, another SN Ia with a prominent high-velocity Si II component, began showing low-velocity Si II (Childress et al. 2013). A similar multi-component velocity structure is evident for the Ca II H&K feature in our pre-maximum spectra.

We fit the early velocity evolution of Ca II H&K and the Si II high-velocity component (the only one we can clearly identify at early times) to a $t^{-0.22}$ power law, as suggested by Piro & Nakar (2013) for finding the explosion time for SNe Ia. To do this, we mimicked the methodology of Piro & Nakar (2014) and allowed the power-law dependence to vary between $t^{-0.20}$ and $t^{-0.24}$ to estimate our uncertainties. This fit implies an explosion on MJD 57821.0 \pm 0.3, 1.1 days prior to discovery and 0.9 days before the implied explosion time from our binary shock + standard SN Ia model presented in §3.

If SN 2017cbv had an SD progenitor, we might expect to see hydrogen in its late-time spectra (Mattila et al. 2005; Leonard 2007; Maeda et al. 2014). However, we do not detect Pa β emission in an NIR spectrum taken 34 days after maximum light (Figure 4, bottom). Following the method of Sand et al. (2016), we calculate a rough limit of $\lesssim 0.1 M_{\odot}$ of hydrogen by comparing to a spectrum of ASASSN-14lp at a similar phase, although this limit depends on the viewing angle.

5. DISCUSSION

The companion-shocking models provide a good fit to our optical data, but not to our UV data. This discrepancy is not likely to be a reddening effect (unless the reddening varies very quickly with time) because the UV luminosities around peak are not unusual for SNe Ia. However, it could stem from several simplifying assumptions in our model:

1. *Blackbody*: The analytic models assume a blackbody spectrum for the shock component. However, the observed spectral energy distribution (SED) during the bump deviates significantly from a blackbody spectrum in the UV (Figure 5). A *Swift* grism spectrum taken during the bump is similar to UV spectra of other SNe Ia, showing significant absorption relative to a blackbody continuum (D.J. Sand et al. 2017, in preparation). This UV suppression is likely due to line blanketing (e.g., from iron lines). Any alternative model, companion shocking or otherwise, will need to account for this deviation from a blackbody spectrum.
2. *Constant Opacity*: We fixed the opacity to be that of electron scattering throughout the first 40 days of evolution, whereas in reality the opacity should change over time as the ejecta cool. Opacity and/or line blanketing that vary with time could potentially explain the discrepancy between the models and our UV data.
3. *Density Profile*: The shock models we quote here assume a broken power-law density profile for the ejecta: $\rho_{\text{inner}} \propto r^{-1}$ and $\rho_{\text{outer}} \propto r^{-10}$. The earliest emission, which should peak in the UV bands, depends strongly on the density of the outermost ejecta layers. In particular, a steeper density profile could suppress the early luminosity.
4. *Spherical Symmetry*: In order to make the problem analytically tractable, we have ignored the asymmetry that must be present in a binary system. The analytic predictions are roughly equivalent to numerical predictions for a favorable viewing angle (see Figure 2 of Kasen 2010). If in reality we are viewing the collision off-axis, we might invoke a larger binary separation, ejecta mass, or ejecta velocity to match our observations. However, 3D numerical modeling of the ejecta-companion interaction would be needed to disentangle the early SN color diversity from the angular dependence of the shock component's color.

If the companion-shocking scenario is correct, but the model is inaccurate in the UV, then the companion sizes found by Marion et al. (2016) and Cao et al. (2015) and the constraints of Brown et al. (2012a) would have to be reevaluated. However, if the UV overprediction is only due to line blanketing, which depends on temperature, the models may be more susceptible to failure in relatively low-temperature events. Alternatively, there could be another cause of early bumps in the UV or optical.

The observed bump could also be interpreted as a collision with CSM, rather than a collision with a companion star, as has recently been modeled by Piro &

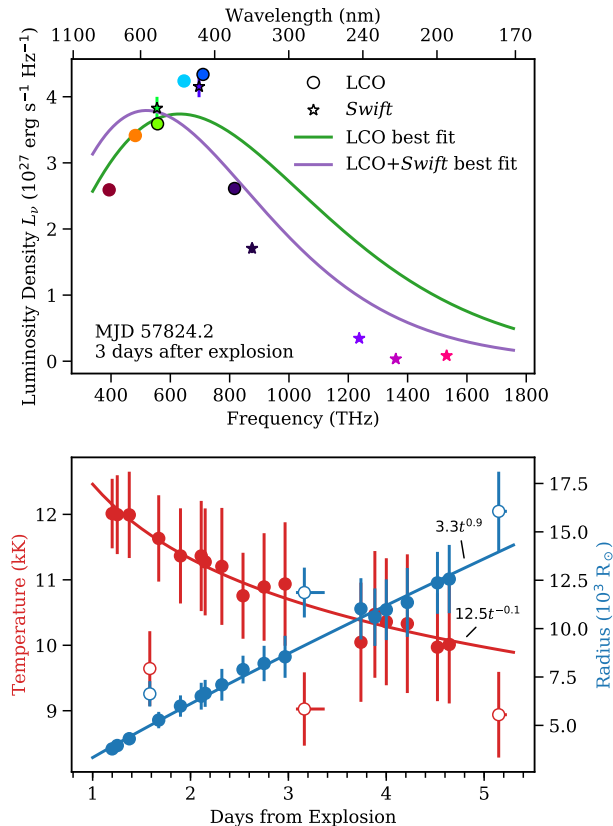


Figure 5. Top: example SED of SN 2017cbv (three days after explosion) and two blackbody fits, with and without the *Swift* observations. Including these filters pulls down the temperature, but neither blackbody spectrum is a good match to the data. Bottom: blackbody temperature and radius evolution of SN 2017cbv during the first five days after explosion, presumably when the shock component dominates the light curve. The filled points use only *UBVgri* data, while the open points include *Swift* photometry. Lines are best-fit power laws, excluding the open points. The temperature evolution may not be reliable, since the SED is not well-described by a blackbody, but the radius evolution is well-constrained and close to what is expected for the Kasen (2010) models ($t^{7/9}$).

Morozova (2016). Kasen (2010) estimates that 0.01–0.1 M_{\odot} of CSM would be needed for a significant effect, and that the material would have to be located at distances comparable to the binary separation. Stellar winds would be unlikely to produce such a configuration, but a DD system could potentially eject enough mass to large enough distances during the pre-supernova accretion phase (Kasen 2010) or during the merger itself (Levanon & Soker 2017). A large mass of CSM would likely have decelerated the ejecta below the velocities we measure in §4, although an unshocked high-velocity component could still persist.

A third possibility is that the bump arises from a bubble of radioactive nickel that escaped most of the ejecta, allowing it to radiate light away faster than the typical diffusion timescale. Piro & Morozova (2016) explored various nickel distributions and their effect on early SN light curves. Shallow nickel distributions result in steeper, bluer early light curves. The early light

curves in Piro & Morozova (2016) that included both CSM interaction and significant nickel mixing bear a qualitative resemblance to the light curve of SN 2017cbv. Likewise, Noebauer et al. (2017) find an early blue bump in their sub-Chandrasekhar double-detonation model, in which the initial helium detonation on the surface produces a small amount of radioactive material. We cannot rule out these possibilities, but more detailed modeling of this event in particular would be necessary to distinguish them from the companion-shocking case.

6. SUMMARY

We have presented early photometry and spectroscopy of the Type Ia SN 2017cbv, which was discovered within ~ 1 day of explosion. Its light curve shows a conspicuous blue excess during the first five days of observations. We find a good fit between our *UBVgri* data and models of binary companion shocking from Kasen (2010), but the fit overpredicts the observed UV luminosity at early times. This discrepancy might be due to several simplifying assumptions in the models. Alternatively, the excess emission could be due to interaction with CSM or the presence of radioactive nickel in the outer ejecta.

We observe no indication of ejecta interaction with hydrogen-rich material stripped from a companion star in the spectra of SN 2017cbv. However, more deep optical and near-infrared spectra out to the nebular phase are needed to confirm this finding. Intriguingly, we do detect unburned carbon in the earliest spectra at a level rarely seen in normal SNe Ia. A connection between an early light curve bump and the presence of unburned carbon could provide an important clue about SN Ia progenitors, but the scarcity of events with either of these observations prevents us from drawing any conclusions now.

Our analysis demonstrates the importance of (1) discovering and announcing SNe as early as possible and (2) obtaining extremely well-sampled follow-up light curves and spectral series. The DLT40 survey and LCO follow-up network are uniquely suited to find very young SNe and follow them with sub-day cadence for long periods. Such observations, which will become increasingly common in the coming years, greatly enhance our ability to confront theoretical models.

We thank Kyle Barbary for his help with *sncosmo* and Alex Conley and Santiago González Gaitán for providing the SiFTO templates. This work makes use of observations from the LCO network as part of the Supernova Key Project. A portion of the *Swift* observations were obtained by time allocated to the Danish astronomy community via support from the Instrument Center for Danish Astrophysics (PI: Stritzinger). G.H., D.A.H., and C.M. are supported by the National

Science Foundation (NSF) under grant No. 1313484. D.J.S. and L.T. are supported by the NSF under grant No. 1517649. Support for S.V. was provided by NASA through a grant (program number HST-GO-14925.007-A) from the Space Telescope Science Institute, which is operated by the Association of Universities for Research in Astronomy, Incorporated, under NASA contract NAS5-26555. Support for I.A. was provided by NASA through the Einstein Fellowship Program, grant PF6-170148. E.Y.H., S.D., and M.S. are supported

by the NSF under grant No. AST-1613472 and by the Florida Space Grant Consortium. M.D.S. acknowledges support by a research grant (13261) from the Villum Fonden. D.J.S. is a visiting astronomer at the Infrared Telescope Facility, which is operated by the University of Hawai'i under contract NNH14CK55B with NASA. This research has made use of the NASA/IPAC Extragalactic Database, which is operated by the Jet Propulsion Laboratory, California Institute of Technology, under contract with NASA.

REFERENCES

- Bianco, F. B., Howell, D. A., Sullivan, M., et al. 2011, *ApJ*, 741, 20
- Bloom, J. S., Kasen, D., Shen, K. J., et al. 2012, *ApJL*, 744, L17
- Breeveld, A. A., Curran, P. A., Hoversten, E. A., et al. 2010, *MNRAS*, 406, 1687
- Brown, P. J., Breeveld, A. A., Holland, S., Kuin, P., & Pritchard, T. 2014, *Ap&SS*, 354, 89
- Brown, P. J., Dawson, K. S., Harris, D. W., et al. 2012a, *ApJ*, 749, 18
- Brown, P. J., Dawson, K. S., de Pasquale, M., et al. 2012b, *ApJ*, 753, 22
- Brown, T. M., Baliber, N., Bianco, F. B., et al. 2013, *PASP*, 125, 1031
- Cao, Y., Kulkarni, S. R., Gal-Yam, A., et al. 2016, *ApJ*, 832, 86
- Cao, Y., Kulkarni, S. R., Howell, D. A., et al. 2015, *Natur*, 521, 328
- Childress, M. J., Scalzo, R. A., Sim, S. A., et al. 2013, *ApJ*, 770, 29
- Conley, A., Sullivan, M., Hsiao, E. Y., et al. 2008, *ApJ*, 681, 482
- Eggleton, P. P. 1983, *ApJ*, 268, 368
- Firth, R. E., Sullivan, M., Gal-Yam, A., et al. 2015, *MNRAS*, 446, 3895
- Foreman-Mackey, D., Hogg, D. W., Lang, D., & Goodman, J. 2013, *PASP*, 125, 306
- Ganeshalingam, M., Li, W., & Filippenko, A. V. 2011, *MNRAS*, 416, 2607
- Ganeshalingam, M., Li, W., Filippenko, A. V., et al. 2012, *ApJ*, 751, 142
- Garavini, G., Folatelli, G., Goobar, A., et al. 2004, *AJ*, 128, 387
- Goobar, A., Kromer, M., Siverd, R., et al. 2015, *ApJ*, 799, 106
- Guy, J., Astier, P., Baumont, S., et al. 2007, *A&A*, 466, 11
- Hayden, B. T., Garnavich, P. M., Kasen, D., et al. 2010, *ApJ*, 722, 1691
- Hossein-zadeh, G., Howell, D. A., Sand, D., et al. 2017, *TNSCR*, 300, 1
- Howell, D. A. 2011, *NatCo*, 2, 350
- Howell, D. A., Sullivan, M., Nugent, P. E., et al. 2006, *Natur*, 443, 308
- Iben, Jr., I., & Tutukov, A. V. 1984, *ApJS*, 54, 335
- Im, M., Choi, C., Yoon, S.-C., et al. 2015, *ApJS*, 221, 22
- Jha, S., Riess, A. G., & Kirshner, R. P. 2007, *ApJ*, 659, 122
- Jordi, K., Grebel, E. K., & Ammon, K. 2006, *A&A*, 460, 339
- Kasen, D. 2010, *ApJ*, 708, 1025
- Kromer, M., Fremling, C., Pakmor, R., et al. 2016, *MNRAS*, 459, 4428
- Kushnir, D., Katz, B., Dong, S., Livne, E., & Fernández, R. 2013, *ApJL*, 778, L37
- Leonard, D. C. 2007, *ApJ*, 670, 1275
- Levanon, N., & Soker, N. 2017, *MNRAS*, 470, 2510
- Liu, Z.-W., Moriya, T. J., & Stancliffe, R. J. 2015, *MNRAS*, 454, 1192
- Maeda, K., Katsuna, M., & Shigeyama, T. 2014, *ApJ*, 794, 37
- Maoz, D., Mannucci, F., & Nelemans, G. 2014, *ARA&A*, 52, 107
- Marion, G. H., Brown, P. J., Vinkó, J., et al. 2016, *ApJ*, 820, 92
- Mattila, S., Lundqvist, P., Sollerman, J., et al. 2005, *A&A*, 443, 649
- Noebauer, U. M., Kromer, M., Taubenberger, S., et al. 2017, arXiv:1706.03613
- Nugent, P. E., Sullivan, M., Cenko, S. B., et al. 2011, *Natur*, 480, 344
- Pakmor, R., Kromer, M., Taubenberger, S., et al. 2012, *ApJL*, 747, L10
- Pan, Y.-C., Foley, R. J., Kromer, M., et al. 2015, *MNRAS*, 452, 4307
- Parrent, J., Friesen, B., & Parthasarathy, M. 2014, *Ap&SS*, 351, 1
- Parrent, J. T., Thomas, R. C., Fesen, R. A., et al. 2011, *ApJ*, 732, 30
- Perlmutter, S., Gabi, S., Goldhaber, G., et al. 1997, *ApJ*, 483, 565
- Phillips, M. M. 1993, *ApJL*, 413, L105
- Piro, A. L., Chang, P., & Weinberg, N. N. 2010, *ApJ*, 708, 598
- Piro, A. L., & Morozova, V. S. 2016, *ApJ*, 826, 96
- Piro, A. L., & Nakar, E. 2013, *ApJ*, 769, 67
- , 2014, *ApJ*, 784, 85
- Poole, T. S., Breeveld, A. A., Page, M. J., et al. 2008, *MNRAS*, 383, 627
- Rabinak, I., Livne, E., & Waxman, E. 2012, *ApJ*, 757, 35
- Rayner, J. T., Toomey, D. W., Onaka, P. M., et al. 2003, *PASP*, 115, 362
- Reichart, D., Nysewander, M., Moran, J., et al. 2005, *NCimC*, 28, 767
- Roming, P. W. A., Kennedy, T. E., Mason, K. O., et al. 2005, *SSRv*, 120, 95
- Sand, D. J., Hsiao, E. Y., Banerjee, D. P. K., et al. 2016, *ApJL*, 822, L16
- Schlafly, E. F., & Finkbeiner, D. P. 2011, *ApJ*, 737, 103
- SDSS Collaboration, Albareti, F. D., Allende Prieto, C., et al. 2016, arXiv:1608.02013
- Shappee, B. J., Piro, A. L., Stanek, K. Z., et al. 2016a, arXiv:1610.07601
- Shappee, B. J., Piro, A. L., Holoien, T. W.-S., et al. 2016b, *ApJ*, 826, 144
- Shen, K. J., & Bildsten, L. 2014, *ApJ*, 785, 61
- Silverman, J. M., & Filippenko, A. V. 2012, *MNRAS*, 425, 1917
- Silverman, J. M., Foley, R. J., Filippenko, A. V., et al. 2012, *MNRAS*, 425, 1789
- Stetson, P. B. 2000, *PASP*, 112, 925
- Tully, R. B. 1988, *Nearby Galaxies Catalog* (Cambridge: Cambridge Univ. Press)
- Valenti, S., Sand, D. J., & Tartaglia, L. 2017, *TNSTR*, 294, 1
- Valenti, S., Howell, D. A., Stritzinger, M. D., et al. 2016, *MNRAS*, 459, 3939
- Webbink, R. F. 1984, *ApJ*, 277, 355
- Whelan, J., & Iben, Jr., I. 1973, *ApJ*, 186, 1007
- Zhang, K., Wang, X., Zhang, J., et al. 2016, *ApJ*, 820, 67
- Zheng, W., Silverman, J. M., Filippenko, A. V., et al. 2013, *ApJL*, 778, L15
- Zheng, W., Shivvers, I., Filippenko, A. V., et al. 2014, *ApJL*, 783, L24
- Zheng, W., Filippenko, A. V., Mauerhan, J., et al. 2017, *ApJ*, 841, 64